PHASE RELATIONS AND CONDUCTIVITY IN THE SYSTEM POLY(ETHYLENE OXIDE)–$LiClO_4$

P. W. M. JACOBS, J. W. LORIMER*, A. RUSSER and M. WASIUCIONEK**

Department of Chemistry, The University of Western Ontario, London, Ont. N6A 5B7 (Canada)

Summary

DSC, DTA, TGA, X-ray, and conductivity measurements have been carried out on mixtures of purified poly(ethylene oxide) (PEO) and lithium perchlorate and the phase diagram of the system PEO + $LiClO_4$ has been determined. The mixtures showed pronounced thermal decomposition beginning at 100 - 150 °C (depending on $LiClO_4$ content) so that phase equilibria could not be determined above the decomposition temperature. The phase diagram indicates the presence of three compounds containing, respectively, one, two, and three Li ions per $-CH_2CH_2O-$ repeating unit. Glass transition temperatures T_g increased with increasing lithium content from 213 K for pure PEO to 269 K at n = 2. Conductivities went through maxima at n = 12 reaching 2.5 × 10^{-3} S cm^{-1} at 373 K. The temperature dependence of conductivity could be represented by the Vogel–Tammann–Fulcher (VTF) equation over the whole temperature range in which the mixtures are amorphous, 298 - 393 K (n = 4, 8), above 313 K (n = 12) or above 323 K (n = 16).

Introduction

This paper is concerned with a detailed characterization of a typical battery electrolyte, the system poly(ethylene oxide)–$LiClO_4$. Among various PEO–lithium salt mixtures, those containing $LiClO_4$ appear to have the highest conductivity [1 - 3]. The equilibrium phase diagram provides information about the temperature and composition regions in which liquid (amorphous) regions occur; it is in these regions that the ionic conductivity is expected to be greatest. For the system PEO–$LiClO_4$, two studies of the phase diagram [2, 4] show significant differences, especially in eutectic composition; doubts have even been expressed if there is eutectic composition [5]. Most published DSC (differential scanning calorimetry) curves

*Author to whom correspondence should be addressed.

**Permanent address: Institute of Physics, Warsaw Technical University, Chodkiewicza 8, 02-525 Warszawa, Poland.

0378-7753/89/$3.50

[4, 6] show thermal effects at temperatures between 220 and 260 K due to glass transitions, and one or two endothermic peaks related to melting appear above 300 K. However, for some compositions, especially at high cooling rates, additional exothermic peaks appear which have been attributed to recrystallization [4, 5].

Not surprisingly, conductivity measurements for this system also show marked differences in dependence on temperature and composition [4, 5, 7 - 9] as large as two powers of ten for comparable conditions. The data have been variously fitted to the Arrhenius equation or to the Vogel–Tammann–Fulcher (VTF) equation [4, 7, 9, 10].

Fauteux *et al.* [11] have reviewed a similar system (NaI–PEO) recently, and have summarized the problems inherent in obtaining reliable measurements: presence of residual water, variations with rates of heating and cooling, and thermal history of the system.

Experimental

Poly(ethylene oxide) (Aldrich, M. W. 4×10^6) contained 1.5 mass % of inorganic ash which by SEM/EDX analysis consisted mainly of Si and Ca. Purification by ion exchange on resins in H^+ and OH^- forms [12], followed by freeze drying, reduced the ash to less than 0.5 mass %, with composition mainly Si, probably as SiO_2.

Differential scanning calorimetry (Perkin-Elmer DSC 1-B) used samples (5 - 12 mg) sealed in aluminum pans inside a dry box flushed with dried, prepurified nitrogen. Measurements were carried out in the low temperature mode from 190 K to 440 K. Usually three determinations were made on each sample at a heating rate of 10 K min^{-1}. The same cooling rate was used. The sample compartment was flushed with dried, prepurified nitrogen at all times.

Complex impedance measurements were made using a Solartron 1250 Frequency Response Analyzer, coupled with a Solartron 1286 Electrochemical Interface, and controlled by a microcomputer. Films of thickness 25 - 150 μm were placed between a pair of stainless steel electrodes of 2 cm^2 surface area in an evacuated glass holder. Before measurement, samples were kept for about 2 h at 90 °C, and were then equilibrated at a given temperature for about 1 h before each measurement. The conductivity was determined from the intercept with the real axis of the linear, low-frequency part of a plot of the imaginary *versus* the real parts of the complex impedance.

X-ray diffraction data were obtained using Cu Kα radiation. Films were mounted on glass slides and sealed from the atmosphere with Mylar film.

Results and discussion

DSC runs for pure PEO and for $(PEO)_n LiClO_4$ with n = 10, 8, 7, 6, and 5 are shown in Fig. 1. The measured melting point of PEO (= A) is 338 K

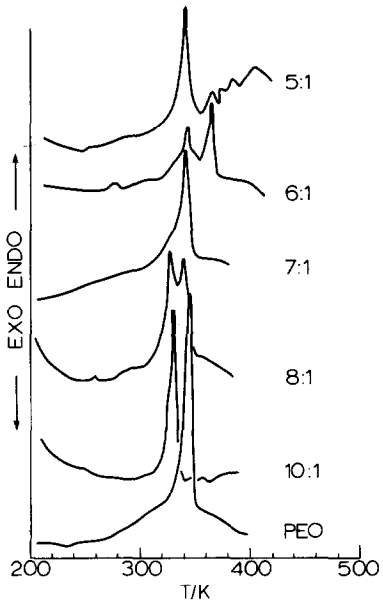

Fig. 1. DSC traces for pure PEO and $(PEO)_n$–$LiClO_4$ with n = 5, 6, 7, 8, 10. Heating rate 10 K min^{-1} under dry N_2; sample size approx. 10 mg.

and the melting curve yields an enthalpy of fusion $\Delta H_{f,A}$ = 5.17 kJ mol^{-1}. The literature value of Gaur and Wunderlich [13] is 8.66 kJ mol^{-1} but ΔH_f depends strongly on the degree of crystallinity. For n = 10, only a single peak is obtained, indicating that this composition must be close to the eutectic composition which, indeed, is at n = 10.9. The eutectic and liquidus peaks are clearly evident in the DSC trace for n = 8, but at n = 7 the eutectic is barely evident as a shoulder, indicating compound formation with composition n = 7. The n = 6 trace shows peritectic and liquidus peaks, the peritectic temperature being 336 K. In general, the first of a pair of endotherms could indicate either eutectic or peritectic behaviour, but the location of this first melting temperature above the liquidus temperature for n = 8 indicates a peritectic, which is confirmed on plotting the complete phase diagram (Fig. 2). For n = 5, we see the peritectic melting of $C_1((PEO)_7LiClO_4)$, but the observation of the liquidus temperature is prevented by superimposed exothermic thermal decomposition. Decomposition is responsible for irreproducible determinations of the liquidus temperature at n = 6 and n = 4.

A particularly clear example of thermal decomposition in PEO + $LiClO_4$ is seen in Fig. 3 for n = 0.26 or x_B = 0.793 (B = $LiClO_4$). The first melting is clearly marked, but is soon totally submerged by a huge exotherm due to decomposition which consumes all the polymer. A second DSC run shows only the melting of excess $LiClO_4$.

The shape of the liquidus peak for n = 6 in Fig. 1 indicates some decomposition, and this is confirmed unambiguously by the TGA and DTA

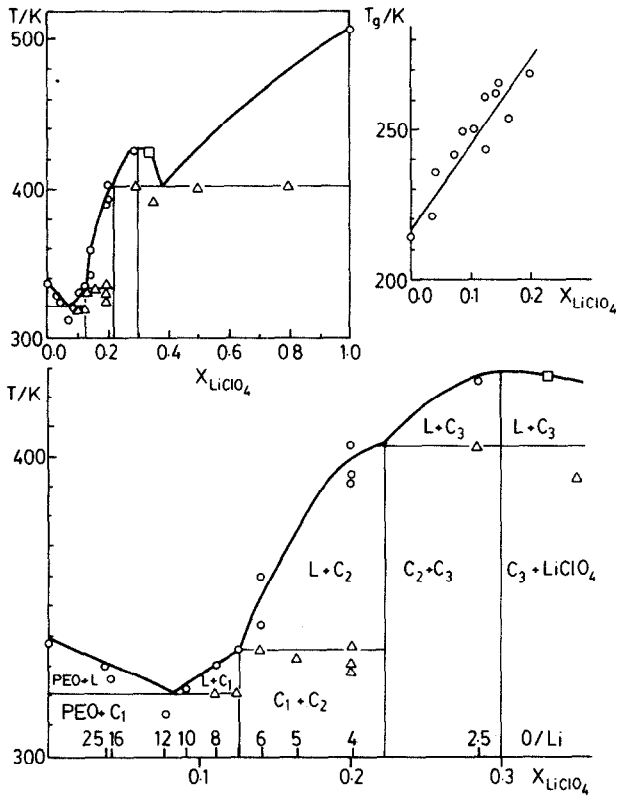

Fig. 2. Calculated phase diagrams of the system PEO + $LiClO_4$. The liquidus lines could not be confirmed experimentally for $x_B > 0.33$ (B = $LiClO_4$), because of decomposition of the polymer–salt mixtures. Experimental results: liquidus temperature: ○, this work; □, from Ferloni *et al.* [4]; △, eutectic or peritectic temperatures.

curves in Fig. 4. Weight loss begins at about 100 °C and at the same time the DTA trace shows pronounced evolution of heat. Even pure PEO shows thermal decomposition above about 185 °C.

The system PEO + $LiClO_4$ shows three distinct temperatures associated with peritectic or eutectic melting, and therefore the system forms three different compounds C_1, C_2, C_3. The dependence of the first observed melting temperature on composition shows that C_2 begins to form at $n > 7$ and C_3 at $n > 3.5$. This suggests the following structural model. PEO adopts a helical configuration and in the crystalline structure there are seven monomer (C_2H_4O) units per unit cell [14]. We suppose that this helical configuration, with a pitch of 1/7, persists even when the phase is amorphous. This regularity of structure encourages a high degree of crystallinity, involving as much as 80% of the polymer lamellae in pure PEO. On adding $LiClO_4$, the Li^+ at first coordinates to one O per unit cell, that is per 360° spiral, forming $C_1 = (PEO)_7LiClO_4$. For $n > 7$, there must be > 1 Li^+ per unit cell and therefore additional interactions (Li^+–Li^+ repulsions as well as increased

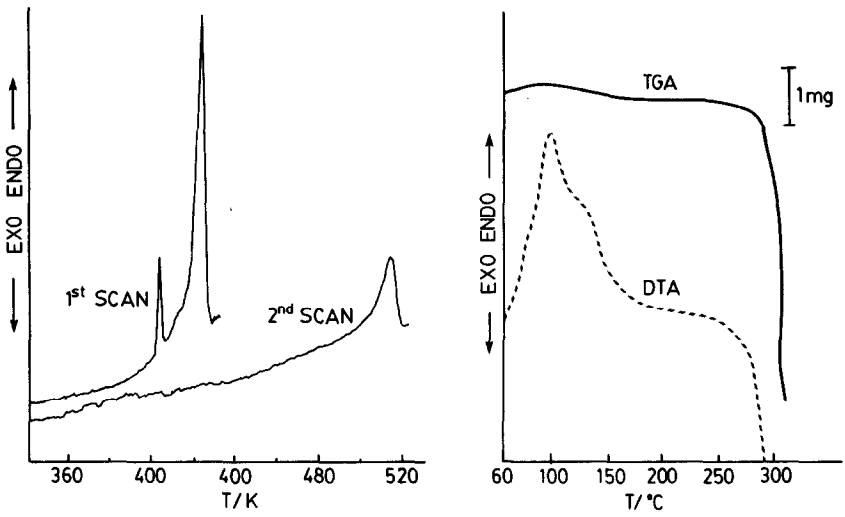

Fig. 3. DSC curves for (PEO)–$LiClO_4$ with $n = 0.26$, $x_B = 0.793$. The first scan shows thermal decomposition, the second melting of residual $LiClO_4$ only.

Fig. 4. TGA and DTA curves for $(PEO)_nLiClO_4$ with $n = 6$. Heating rate 10 K min^{-1} under dry argon; sample size 67 mg.

Li^+–O binding), so that a new compound $C_2 = (PEO)_7(LiClO_4)_2$ forms. This is stable up to $x_B = 0.222$ or $n = 3.5$; at higher Li^+ concentrations there must be 3 Li^+ per complete spiral and $C_3 = (PEO)_7(LiClO_4)_3$ begins to form. This is the maximum amount of Li^+ that can bond to PEO without having Li^+ ions bonded to nearest-neighbour O atoms, an unstable configuration because of strong Li^+–Li^+ repulsions. For $x_B > 0.3$ the excess $LiClO_4$ exists as $LiClO_4$ and no new compounds form (for example, at $n = 7/4$, $x_B = 0.364$), as shown by the constant first melting temperature for $0.3 < x_B < 1$.

We may now deduce the phase diagram for PEO + $LiClO_4$ expected from this model. For the equilibrium (A = PEO, B = $LiClO_4$)

$$nA(l) + B(l) = A_nB(s) \tag{2}$$

$$\ln[(1 - x_B)^n x_B] = \ln[n^n/(n+1)^{n+1}] - (\Delta H_{f,A_nB}/R)(1/T - 1/T^*_{f,A_nB}) \tag{3}$$

where $T^*_{f,i}$ is the melting point of pure i, and it has been assumed that the activity coefficients have the same dependence on temperature as the solubilities and that the salt is not ionized. The liquidus lines for $0.082 < x_B < 0.38$ in Fig. 2 have been calculated from eqn. (3) with $n = 7$, 3.5, and 2.33, using enthalpies of fusion, ΔH_f, estimated from the eutectic or peritectic points and the melting points of C_1, C_2, C_3 (Table 1). For the PEO-rich and $LiClO_4$-rich branches the equations are:

$$\ln x_i = -(\Delta H_{f,i}/R)(1/T - 1/T^*_{f,i}) \tag{4}$$

with i = A, B. $\Delta H_{f,A}$ was determined experimentally by DSC and $\Delta H_{f,B}$ from the (calculated) eutectic composition and the measured melting temperature of $LiClO_4$. The calculated phase diagram is in excellent agreement with our experimental data showing the basic correctness of our structural model. We also used one point from ref. 4 to help fix the melting point of C_3 more precisely. Other phase diagrams in the literature show many features that are approximately correct, but the complete phase diagram has not been elucidated previously, although the existence of crystalline complexes with different values of n has been noted [2]. At all compositions, cooling of melts at 10 K min^{-1} produced a glass, which crystallized at a temperature just below the eutectic on immediate heating at 10 K min^{-1}, or by annealing at temperatures as low as 260 K for 1 h, except at the eutectic composition, where recrystallization was very slow. The glass transition temperatures (Fig. 2) vary from 213 K for pure PEO to 269 K at x_B = 0.3, agree well with those reported in ref. 1, and increase with salt content, especially at low mole fractions of $LiClO_4$.

TABLE 1

Thermal data used in construction of the phase diagram for PEO(A)–$LiClO_4$(B)

n	$\Delta H_{f,A_nB}$ (kJ mol^{-1})	T (K)
∞	5.17	338 melting point, pure A
10.9	—	321 eutectic
7	4.35	336 peritectic
3.5	2.29	404 peritectic
2.33	2.67	429 peritectic
0	15.5	509 melting point, pure B

X-ray diffraction measurements (Fig. 5) provide qualitative confirmation of the formation of new compounds as n decreases. No sharp lines are seen at all but the PEO film shows evidence of 3 diffraction regions not present in the Mylar window. For n = 10 new diffraction peaks due to C_1 appear. These peaks persist down to n = 8, but at n = 7 new peaks due to C_2 arise. These grow in intensity at the expense of those due to C_1 until, at n = 5, the C_2 peaks dominate the spectrum. No measurements were made at lower n, but the results of Robitaille and Fauteux [2] clearly show the presence of a third compound (C_3) at n = 2. The model also accounts satisfactorily for the three kinds of spherulites observed by Neat *et al.* [10] at mole fractions x_B = 0.08, 0.17 and >0.2.

The conductivity, σ, of $(PEO)_n \cdot LiClO_4$, for n = 2.5, 4, 8, 12, 16, and 25 was measured as a function of T at decreasing temperatures after prior annealing at 380 K. For n = 2.5, σ was at least two orders of magnitude lower than that for n = 4, and obeyed the Arrhenius equation. Reference

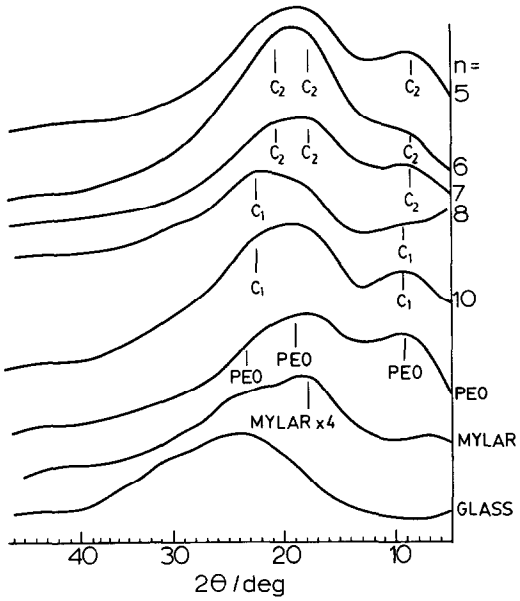

Fig. 5. X-ray diffraction spectra for a glass slide used to support films, for 4 thicknesses of Mylar window on the glass slide, and for films of pure PEO and of $(PEO)_nLiClO_4$ with n = 5, 6, 7, 8, and 10.

to Fig. 2 shows that the sample was unmelted, and consisted of a mixture of the solid phases C_2 and C_3. For n = 4 and 8, σ obeyed the VTF equation: $\ln(\sigma T^{1/2}) = \ln A - E/R(T - T_0)$ in the range 380 - 295 K, which is consistent with a liquid polymer, or a mixture of liquid and amorphous phases, or of two amorphous phases. For n = 16, for which the mole fraction of $LiClO_4$ (x = 0.059) is decidedly less than that at the eutectic composition (x = 0.083), the conductivity obeys the VTF equation in the range 390 - 322 K, but at lower temperatures, σ is much smaller than the values predicted by extrapolating the VTF equation fitted to the high temperature data. This shows that at sufficiently high PEO concentrations (greater than the eutectic composition) PEO begins to crystallize out below the liquidus line. Repeat DSC scans (Fig. 6(a)) show no evidence of crystallization on heating previously melted samples, and thus imply the presence of two solid phases, one of which is crystalline PEO and the other phase C_1. The conductivity of samples with n = 25 behaved similarly, with the onset of crystallization evident at 328 K, in good agreement with the phase diagram. There was again no evidence in repeat DSC scans of recrystallization prior to melting.

The rather complex dependence of the conductivity of $(PEO)_n \cdot LiClO_4$ on temperature and composition is thus in complete accord with our model and with the phase diagram deduced from this model. For n = 12, the concentration of PEO is just greater than that corresponding to the eutectic

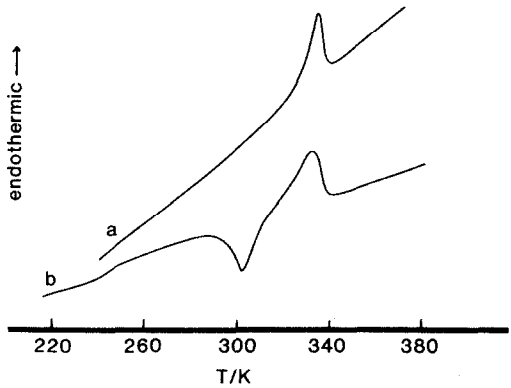

Fig. 6. DSC curves obtained in repeat runs on previously-melted samples. Otherwise, conditions were as for the curves in Fig. 1. (a) $(PEO)_{16}\cdot LiClO_4$, showing that no recrystallization occurs prior to melting; $(PEO)_{25}\cdot LiClO_4$ behaved similarly. (b) $(PEO)_{12}\cdot LiClO_4$, showing an exothermic recrystallization peak just prior to the eutectic temperature. The glass transition at 242 K is also clearly evident.

temperature, and so one might expect, as confirmed by the work of Neat *et al.* [10], a partly crystalline, partly amorphous PEO phase, together with amorphous C_1. Recrystallization of the PEO just prior to melting is clearly evident in Fig. 6(b).

Acknowledgement

This work was supported by the Natural Sciences and Engineering Research Council of Canada under a Strategic Grant (G1651).

References

1 J. M. Chabagno, *Thèse de Doctorat*, Grenoble, 1980.
2 C. D. Robitaille and D. Fauteux, *J. Electrochem. Soc.*, *133* (1986) 315.
3 E. A. Rietman, M. L. Kaplan and R. J. Cava, *Solid State Ionics*, *17* (1985) 67.
4 P. Ferloni, G. Chiodelli, A. Magistris and M. Sanesi, *Solid State Ionics*, *18/19* (1986) 265.
5 C. Berthier, W. Gorecki, M. Minier, M. B. Armand, J. M. Chabagno and P. Rigaud, *Solid State Ionics*, *11* (1983) 91.
6 W. Gorecki, R. Andreani, C. Berthier, M. Armand, M. Mali, J. Roos and D. Brinkmann, *Solid State Ionics*, *18/19* (1986) 295.
7 P. R. Sørensen and T. Jacobsen, *Solid State Ionics*, *9/10* (1983) 1147.
8 A. Bouridah, F. Dalard, D. Deroo and M. B. Armand, *Solid State Ionics*, *18/19* (1986) 287.
9 J. E. Weston and B. C. H. Steele, *Solid State Ionics*, *7* (1982) 81.
10 R. J. Neat, A. Hooper, M. D. Glasse and R. G. Linford, in I. W. Powlsen (ed.), *6th RISØ Int. Symp. Metallurgy*, RISØ Int. Lab., Denmark, 1985, p. 341.
11 D. Fauteux, M. D. Lupien and C. D. Robitaille, *J. Electrochem. Soc.*, *134* (1987) 2761.
12 R. Dupon, D. H. Whitmore and D. F. Shriver, *J. Am. Chem. Soc.*, *128* (1981) 715.
13 U. Gaur and B. Wunderlich, *J. Phys. Chem. Ref. Data*, 10 (1981) 1001.
14 M. B. Armand, in J. R. MacCallum and C. A. Vincent (eds.), *Polymer Electrolyte Reviews*, Vol. 1, Elsevier, London, 1987, p. 1.